Facile Co 3 O 4 nanoparticles deposited on polyvinylpyrrolidine for efficient water oxidation in alkaline media

Abdul Qayoom Mugheri, Aneela Tahira, Umair Aftab, Ayman Nafady, Brigitte Vigolo, Zafar Hussain Ibupoto

Facile Co_3O_4 nanoparticles deposited on polyvinylpyrrolidine for efficient water oxidation in alkaline media

Abdul Qayoom Mugheri[a], Aneela Tahira[a], Umair Aftab[b], Ayman Nafady*[c], Brigitte Vigolo[d], Zafar Hussain Ibupoto*[a]

[a] Dr. M.A Kazi Institute of Chemistry University of Sindh Jamshoro, 76080, Sindh Pakistan

[b]Department of Metallurgy and Materials Engineering, Mehran University of Engineering and Technology, 7680 Jamshoro, Sindh Pakistan

[c]Department of Chemistry, College of Science, King Saud University, Riyadh 11451, Saudi Arabia

[d]Université de Lorraine, CNRS, IJL, F-54000 Nancy, France

*__Corresponding authors__. Prof. Zafar Hussain Ibupoto, Email: zaffar.ibhupoto@usindh.edu.pk,

Abstract

To develop an inexpensive, earthabundant, efficient, and stable catalyst is very crucial for the realization of renewable energy for practical applications, but it is a difficult task. In this research study, we have deposited Co_3O_4 nanoparticles on polyvinylpyrrolidine (PVP) through electro-spun technique followed by carbonization. The structure and composition studies were carried by scanning electron microscopy (SEM), energy dispersive spectroscopy (EDS), and powder X-ray diffraction (XRD) techniques. The Co_3O_4 nanoparticles are deposited on the nanofibers of PVP with improved surface area and conductivity, therefore the hybrid material has shown an excellent oxygen evolution reaction (OER) in alkaline media. The onset potential for the presented OER catalyst is about 1.46 V versus reversible hydrogen electrode (RHE) and an overpotential of 280 mV is needed to reach a current density of 10 $mAcm^{-2}$. The Co_3O_4 nanoparticles are highly durable for 20 hrs and very stable. The low charge transfer resistance of 29.23 Ohms is offered by the Co_3O_4 hybrid material which facilitated the OER kinetics in alkaline media. These obtained OER

results may be utilized for the overall water splitting and the synthetic strategy is low cost, thus it favors the mass production of functional materials for diverse electrochemical applications.

Keywords. Carbonized Co_3O_4 nanoparticles, polyvinylpyrrolidone, oxygen evolution reaction.

1. Introduction

The water splitting reaction on the surface of electrocatalyst describes the [$H_2O \rightarrow O_2 + 2H_2$] production of hydrogen and oxygen gases and it is considered one of the potential strategies for the generation of green H_2 and O_2 based fuels renewable energy applications [1, 2]. Unfortunately, the big barrier in water electrolysis is oxidation reaction at the anode which consumes large overpotential and it demonstrates a dead kinetics for the oxygen evolution reaction (OER) as OER process is followed by the four-electron transfer [3, 4, 5]. For this reason, numerous research activities have been carried out for the design of highly active electrocatalysts with a low overpotential and enhanced OER kinetics [6]. The noble materials like RuO_2 and IrO_2 have been testified so far as efficient OER electrocatalysts to date [5]. Inherently, these precious materials are limited in use at large scale due to their high cost, scarcity, and poor chemical stability in basic media. The development of new nonprecious catalysts for OER application, it is highly needed to consider the cost of fabrication to capitalize them for industrial applications. At the present, we have only Ir/Ru based materials as efficient towards OER, however they are restricted by their high cost. Therefore, it is very important to develop and fabricate a nonprecious, earth abundant and efficient OER electrocatalysts. For this purpose, an intense progress has been made for the synthesis of earth abundant and low cost OER electrocatalysts [7, 8]. Despite this, more facile and low-cost techniques are needed for the fabrication of active electrocatalysts based on earth abundant materials. The use of first 3d series transition metal based electrocatalysts has been considered at large extent for the OER application due to their low cost, earth abundance and tunable 3d electronic properties [9]. These 3d transition metal-based compounds are utilized in OER catalysis in different forms such as metal oxides [10, 11], perovskites [12], metal oxy/hydroxides [13,14], metal phosphates [15], and organic frameworks [16]. Among them, cobalt oxide Co_3O_4 in spinel structure is of high importance due to its unique properties like high activity [17], significant stability [18], and very suitable over wide range of electrolytic pH [19]. Also, Co_3O_4 is low-cost material and has high abundance in nature. The use of Co_3O_4 as OER electrocatalyst with large surface area and high-density active sites is appreciated by the scientific

community as it favors Co_3O_4 for practical applications. Various synthetic methods have been used to produce nanostructured Co_3O_4 including hydrothermal [20], casting [21] and plasma engraving [22]. The Co_3O_4 has been produced into various morphologies like nanowires/nanorods, nanofibers, nanotubes, nanoparticles, nanoflakes and nanosheets through wet chemical and electrochemical methods [23-26]. Moreover, the electro-spinning method is promising for the preparation of nanostructured materials like nanofibers which accelerate the ion mobility between electrode-electrolyte interfaces [27] due to their large surface area and porosity. The electro-spinning technique has been used for the preparation of Co_3O_4 onto polyvinylpyrrolidone (PVP) fibers to produce composite nanostructure for oxygen reduction reaction [28]. The electro-spun composite nanostructure of RuO_2–Co_3O_4 has been reported with improved catalytic activity for the oxygen reduction reaction [29]. The work is novel in terms of functional properties by demonstrating the OER activity in alkaline media for the first time on cobalt oxide nanoparticles deposited on PVP fibers followed by carbonization. Also, the used strategy is facile, low cost, environment friendly and highly suitable from mass production of functional materials for the diverse electrochemical applications. In this study, we present a simple methodology for the synthesis of OER electrocatalyst using PVP carbon nanofibers as a carbonized source for the deposition of Co_3O_4 nanoparticles by electro-spinning method. The Co_3O_4 nanoparticles are characterized by XRD, SEM, and EDs techniques. These nanostructured showed an enhanced OER activity in 1.0M KOH with an overpotential of 280 mV for 10 $mAcm^{-2}$. Also, the composite catalysts are durable for 20 hrs.

2. Experimental Section

The Cobalt nitrate hexahydrate, polyvinylpyrrolidine PVP, 20% RuO_2/C and ethanol were received from Sigma Aldrich Karachi Pakistan. The chemicals were used as received. The Co_3O_4 nanoparticles were deposited on PVP nanofibers by electro-spinning method and a detail methodology is as described. The PVP fibers were produced according to the reported work [30]. First, 0.4g of cobalt nitrate hexahydrate were mixed in 1.6 mL of H_2O and 0.4 g of PVP in 2.4 mL of ethanol. Both solutions were kept on stirring for 2 h, then mixed. Then a 19-gauge needle was filled with this solution and electro-spun was performed at the flow rate of 0.3 mL/h at 20 kV with separation distance of 15 cm. The nano fibers product was deposited on the aluminum foil and thermally treated at 500 ^oC for 5 hrs in air to get carbonized Co_3O_4 nanoparticles. . The pristine

Co_3O_4 nanostructures were prepared by hydrothermal method using equ-molar concentration (0.1M) of cobalt nitrate hexahydrate and urea at 90 ^oC for 5 hrs. Afterwards calcination was performed at 500 ^oC for 5 hours in air. The composition and crystalline structure were studied on Philips's powder diffractogram technique using CuKα radiation (λ = 1.5418 Å), 45 kV and 45 mA. The SEM measurement was done at at 3 kV and' to ' Scanning electron microscopy was carried out with a ZEISS Gemini SEM 500 equipped with field emission gun.

2.1. Electrochemical experiments

The carbonized Co_3O_4 nanoparticles were used to modify glassy carbon electrode (GCE). The GCE was rubbed with 1µm and 0.05 µm alumina pastes then washed with water. Then sonication was performed on the GCE and rinsed several times with ethanol and left to dry at room temperature. The geometrical surface area of 0.021 cm^2 of GCE was used. The catalyst slurry was as prepared by mixing 5mg/ml of each material such as Co_3O_4 carbonized Co_3O_4 nanoparticles and pristine Co_3O_4 in 0.8 mL of ethanol and mechanically stirred then a 5µl of 5% Nafion were added as binder. Afterwards, 5µL of catalyst was deposited on GCE with a mass of (0.2mg) and dried at room temperature. The use of carbonized Co_3O_4 nanoparticles and pristine Co_3O_4 catalyst ink onto the glassy carbon electrode was done separately. The electrochemical measurements were performed on three electrode setup including graphite rod as counter electrode, silver-silver chloride as reference electrode and catalyst modified GCE as working electrode. The cyclic voltammetry (CV) was used to stabilize the working electrode prior to linear sweep voltammetry (LSV). The LSV was performed at scan rate of 1 mV/s in 1.0M KOH the EIS spectra were recorded from 100 kHz to 1Hz using sinusoidal potential 5 mV and 1.51 V vs RHE in 1.0M KOH. All the potential is converted into RHE using Nernst equation. For the calculation of current density, the measured current was divided by the geometrical surface area of GCE. For better understanding, a brief schematic diagram illustrating the synthesis process and electrochemical analysis is shown in Figure 1.

3. Results and discussion

To analyze the morphology of different nanostructured materials via scanning electron microscopy (SEM) as enclosed in Figure 2. It is found that the nanofibers of PVP are successfully formed as

shown in Figure 2c. They are decorated with the nanoparticles of Co_3O_4 and exhibit a dimension of several microns and an average diameter of 300-500 nm as shown in Figure 2b. The pristine Co_3O_4 possessed a plate like morphology as shown in Figure 2a. The XRD analysis was carried on the pristine Co_3O_4 and carbonized Co_3O_4 nanoparticles and the prominent diffraction patterns 111, 022, 113, 222, 004, 133, 224, 115, 044, 135, 244, 026, 335, and 226 were found as enclosed in Figure 2d. The XRD results of both pristine Co_3O_4 and carbonized Co_3O_4 nanoparticles are consistent with the reference card no. 96-900-5895. No another suspicious or impurities were identified by XRD measurement. The chemical composition analysis by EDS shows that a quantified amount of 4.3% of carbon is present in the composite samples which revealed the existence of carbon from PVP fibers as shown in Figure 3. An impurity of Sn was found which appeared from the fluorine doped tin oxide substrate on which analysis was carried out. The Co and O are the main elements in the sample as described in Figure 3. The carbonized Co_3O_4 nanoparticles have enhanced conductivity and surface area which favored an efficient OER kinetics.

The OER activity of carbonized Co_3O_4 nanoparticles, bare PVP fibers, 20%RuO_2/C and pristine Co_3O_4 was tested in 1.0 M KOH electrolyte using three electrodes set up as shown in Figure 4a. The LSV polarization curves were measured for the pristine Co_3O_4, carbonized Co_3O_4 nanoparticles, bare PVP and 20%RuO_2/C. It is highly needed to design nonprecious OER catalysts with a low overpotential. The pristine Co_3O_4 nanoparticles are experienced by large over potential due to their poor electrical conductivity and a smaller number of catalytic sites. Pristine Co_3O_4 showed a poor activity, however the carbonized Co_3O_4 nanoparticles have improved the catalytic performance with an overpotential of 280 mV to produce a 10 $mAcm^{-2}$. The use of PVP fibers as a carbonized source not only increased the electrical conductivity of Co_3O_4 nanoparticles but it also has lifted uniform dispersion of Co_3O_4 nanoparticles, and exposed of large number of active sites, thus an enhanced OER activity is demonstrated. The bare PVP fibers are found catalytic inactive; therefore, they only provided a high surface area to the Co_3O_4 nanoparticles. The inactivity of PVP fibers shows that the OER activity is mainly coming from the Co_3O_4 nanoparticles, and it could be safe to say that the increase in the surface area for a metal oxide nanostructure may have high potential to accelerate the OER kinetics. The meritorious activity of 20%RuO_2/C was observed with an overpotential 160 mV to reach a 10 $mAcm^{-2}$. As, it is well known that the RuO_2 being a noble catalyst is limited by the widespread use due to its high cost

and rare abundance. However, the carbonized Co_3O_4 nanoparticles being a low cost, earth abundant and improved OER activity can be used at large scale for practical applications. The scale up features of proposed material can be capitalized for the overall water splitting. The superior OER performance of carbonized Co_3O_4 nanoparticles might be assigned to their high surface to volume ratio, excellent conductivity, and fast diffusion of electrolyte. The OER kinetics is well explained by the Tafel plots extracted from the linear region of LSV curves. From Figure 4b, it is obvious that RuO_2 exhibited a lower Tafel value of 55 $mVdec^{-1}$compared to our Co_3O_4 hybrid material 96 $mVdec^{-1}$. The proposed hybrid material is nonprecious, and the obtained Tafel slope is still low and acceptable which highlight the favorable OER kinetics. The Tafel slope value of Co_3O_4 hybrid material is comparable to the recently reported results [31]. The pristine Co_3O_4 possess a Tafel slope of 103 $mVdec^{-1}$ which is bit higher compared to the Co_3O_4 composite material. This illustrates that the PVP nanofibers improved OER kinetics of Co_3O_4 by providing large surface area and improved the conductivity of Co_3O_4 through carbonization. The Tafel plotting is used to understand the limiting mechanism of the electrochemical process. The OER kinetics on the surface of Co_3O_4 composite, systems were evaluated by Tafel plots under alkaline conditions. The Co_3O_4 composite material exhibits a low Tafel slope as compared to pristine Co_3O_4 and PVP. The OER mechanism is not well understood in the literature, however, it involves the 4-electron transfer process, thus considered kinetically sluggish. Generally, the Tafel value of 120 $mVdec^{-1}$ indicates the limiting path involving a first electron transfer step, the slope of 60 $mVdec^{-1}$ is revealing that kinetics is controlled by the adsorption, whereas the Tafel slope of 40 $mVdec^{-1}$ is involving the second electron transfer step [32, 33, 34]. The Tafel slope of Co_3O_4 hybrid material is suggesting the OER kinetics followed by the chemical step. The long-term usability of nonprecious catalyst is a big challenge and we investigated it at constant current density.

The durability experiment was performed on the Co_3O_4 composite material using chronopotentiometry test at a constant current density of 20 $mAcm^{-2}$ for 20 h as shown in Figure 4c. The durability test has verified the stationary state of the catalyst without any drop of the potential; however, some fluctuation could be seen due to the bubbling of oxygen gas. The negligible loss of potential at constant current density suggests that the Co_3O_4 composite material has high potential for practical applications especially in water electrolyzer. To support the durability results, we measured the LSV curves before and after the durability test and observed

no decay in the onset potential as shown in Figure 4d. The stability experiment indicates that the composite material has maintained the overpotential even after the durability test for 20 h.

It has been believed that the activity of a catalytic material is linearly related to the density of active sites and the intrinsic characteristic of individual active site. For this purpose, the electrochemical double layer capacitance (Cdl) which is inherently associated to the electrochemical active surface area (ECSA) was quantified by the CV study at different scan rates in non-Faradic region as shown in Figure 5 [35]. It can be seen from Figure 5c the Cdl of pristine Co_3O_4 is 11.9 $\mu F\ cm^{-2}$ and Co_3O_4/PVP is 26.4.9 $\mu F\ cm^{-2}$. It is obvious that the carbonized Co_3O_4 nanoparticles exhibit a double value of Cdl and it suggests that the more density of catalytic sites are produced in the composite material and it highlights the scientific reason for the improved OER performance.

To access the deeper insight into the improved catalytic performance of Co_3O_4 composite material, the electrochemical impedance spectra were recorded for the frequency 100 kHz to 1Hz at OER at a potential of 1.51 V versus RHE as shown in Figure 6. Figure 6a, b shows the Bode plots which indicate the low resistance in the film of Co_3O_4 composite compared to the pristine Co_3O_4. Figure 6c shows the Nyquist plots for the Co_3O_4 composite and pristine Co_3O_4 which again confirms the low charge transfer offered by the Co_3O_4 hybrid material during the OER process and these observations supports the claims made on the LSV results. The simulated impedance results for the circuit elements are given in Table 1. The Co_3O_4 hybrid material bears a low charge transfer resistance of 29.23 Ohms which is three times lower than the pristine Co_3O_4 94.98 Ohms, thus it explains the reason for the outperform performance of Co_3O_4 hybrid material. The results of impedance are strongly supported by the reported studies [36, 37]. The capacitance double layer value of 1.11 mF was also found for the Co_3O_4 hybrid material which is higher than the pristine Co_3O_4 0.68 mF. The OER performance of Co_3O_4 composite was also compared with already reported OER catalysts as given in Table 2. The OER activity of Co_3O_4 composite material is better in terms of low overpotential compared to the published results.

4. Conclusions

In summary, we have deposited Co_3O_4 nanoparticles on PVP fibers via electro-spun method followed by carbonization. The prepared materials of Co_3O_4 are well characterized by SEM, EDS and XRD. The high surface area and enhanced conductivity of Co_3O_4 composite due to carbonization have made an advancement in the design of efficient nonprecious electrocatalyst for OER in 1.0M KOH aqueous solution. The Co_3O_4 composite exhibited a low overpotential of 280 mV at 10 $mAcm^{-2}$. Also, they showed a Tafel slope of 96 $mVdec^{-1}$. Furthermore, EIS analysis described the low charge transfer resistance of 29.23 Ohms for the Co_3O_4 composite and it confirms the faster charge transport during electrochemical reaction. These results motivate that the carbonized Co_3O_4 nanoparticles are the potential materials for several applications particularly in the field of energy and environment sciences.

5. Acknowledgment

We extend our sincere appreciation to the Researchers Supporting Project number (RSP-2021/79) at King Saud University, Riyadh, Saudi Arabia. We also, would like to thank the platform "Microscopies, Microprobes and Metallography (3M)" (Institut Jean Lamour, IJL, Nancy, France) for access to SEM facilities.

6. Conflict of interest

Authors declare no conflict of interest in this study

7. References

1. Ghribi D, Khelifa. A, Diaf. S, et al. Study of hydrogen production system by using PV solar energy and PEM electrolyser in Algeria. Int. J. Hydrogen Energy 2013; 38 (20):8480-8490.
2. Yongtao. M, Wenqiao S, Hui H, Zheng R, et al. Structure–property relationship of bifunctional MnO2 nanostructures: highly efficient, ultra-stable electrochemical water oxidation and oxygen reduction reaction catalysts identified in alkaline media Chem. Soc. 2014; 136 (32):11452-11464.
3. Bediako D K, Surendranath, Nocera D G, Mechanistic studies of the oxygen evolution reaction mediated by a nickel–borate thin film electrocatalyst. J. Am. Chem. Soc. 2013; 135 (9):3662-3674.
4. Seitz L C, Hersbach T J, Nordlund D, et al. Enhancement Effect of Noble Metals on Manganese Oxide for the Oxygen Evolution Reaction. J. Chem. Lett. 2015; 6 (20):4178-4183.

5. Siracusano S, Van D N, Johnson E P, et al. Nanosized IrOx and IrRuOx electrocatalysts for the O2 evolution reaction in PEM water electrolysers. J. Appl. Catal. B-Environ. 2015; 164: 488-495.
6. Katsounaros I, Cherevko S, Zeradjanin A R, et al. Oxygen electrochemistry as a cornerstone for sustainable energy conversion. J. Angew. Chem. Int. Ed 2014; 53(1): 102-121.
7. Bajdich M, García-Mota M, Vojvodic A, et al. Theoretical investigation of the activity of cobalt oxides for the electrochemical oxidation of water. J. Am. Chem. Soc. 2013; 135 (36): 13521-13530.
8. Sheng H, Erick L, Ribeiro, et al. MOF-derived PtCo/Co_3O_4 nanocomposites in carbonaceous matrices as high-performance ORR electrocatalysts synthesized *via* laser ablation techniques. RSC Adv. 2017; 7 33166-33176.
9. Rosen J, Hutchings G S, & Jiao F, Ordered Mesoporous Cobalt Oxide as Highly Efficient Oxygen Evolution Catalyst. J. Am. Chem. Soc. 2013; 135 (11): 4516-4521.
10. Wei-Yan X, Nan L, Qing-Yu, et al. Au-NiCo_2O_4 supported on three-dimensional hierarchical porous graphene-like material for highly effective oxygen evolution reaction. J. *Sci. Rep*. 2016; 6 23398.
11. Zhuang Z, Sheng W, & Yan Y. Sea urchin-like cobalt–iron phosphide as an active catalyst for oxygen evolution reaction. J. Adv. Mater 2014; 26:3950-3955.
12. Chai H, Peng X, Liu T, Su X, Jia D, & Zhou W, High-performance supercapacitors based on conductive graphene combined with Ni (OH) 2 nanoflakes. RSC advances. 2017; 7(58), 36617-36622.
13. Roger I, Shipman M A, Symes M D, Earth-abundant catalysts for electrochemical and photoelectrochemical water splitting. J. Nat. Rev. Chem 2017; 1 (1): 013-21.
14. Deng X, Tüysüz H, Water oxidation catalysis beginning with 2.5 μM [Co4 (H2O) 2 (PW9O34) 2] 10–: Investigation of the true electrochemically driven catalyst at≥ 600 mV overpotential at a glassy carbon electrode. J. ACS Catal. 2014; 3 (6): 1209–1219.
15. Song F, Bai L, Moysiadou A, et al. Transition metal oxides as electrocatalysts for the oxygen evolution reaction in alkaline solutions: an application-inspired renaissance. J Am. Chem. Soc 2018; 140 (25): 7748-7759.
16. Suntivich J, May K J, Gasteiger H A, et al. A perovskite oxide optimized for oxygen evolution catalysis from molecular orbital principles. J. Science 2011; 334 (6061): 1383-1385.

17. Moon G h, Yu M, Chan C K, et al. Highly Active Cobalt-Based Electrocatalysts with Facile Incorporation of Dopants for the Oxygen Evolution Reaction. J. Angew. Chem. Int. Ed. *131*(11): 3529-3533.
18. Trotochaud L, Young S L, Ranney J K, et al. Nickel–iron oxyhydroxide oxygen-evolution electrocatalysts: the role of intentional and incidental iron incorporation. J. Am. Chem. Soc. 2014: 136 6744-6753.
19. Menezes P W, Indra A, Zaharieva I, Walter C, et al. Helical cobalt borophosphates to master durable overall water-splitting. J. Energy Environ. Sci. 2019;12 (3): 988-999.
20. Xia B Y, Yan Y, Li N, Wu H B, et al. Embedding CoS2 nanoparticles in N-doped carbon nanotube hollow frameworks for enhanced lithium storage properties. J. Nat. Energy 2016 1 1500621.
21. McCrory C C L, Jung S, Ferrer I M, et al. Benchmarking hydrogen evolving reaction and oxygen evolving reaction electrocatalysts for solar water splitting devices. J. Am. Chem. Soc. 2015; 137 (13): 4347-4357.
22. Ma T Y, Dai S, Jaroniec M, et al. Metal-organic framework derived hybrid Co3O4-carbon porous nanowire arrays as reversible oxygen evolution electrodes. J. Am. Chem. Soc. 2014 136 (39):13925-13931.
23. Gerken J B, McAlpin J G, Chen J Y C, et al. Electrochemical water oxidation with cobalt-based electrocatalysts from pH 0–14: the thermodynamic basis for catalyst structure, stability, and activity. J. Am. Chem. Soc 2011; 133 (36):14431-14442.
24. Xia X H, Tu J P, Mai, Y J, et al. Self-supported hydrothermal synthesized hollow Co3O4 nanowire arrays with high supercapacitor capacitance. J. Mater. Chem. 2011; 21 (25): 9319-9325.
25. Grewe T, Deng X, Weidenthaler C, et al. Development of Highly Active Bifunctional Electrocatalyst Using Co3O4 on Carbon Nanotubes for Oxygen Reduction and Oxygen Evolution. J. Chem. Mater. 2013; 25 4926-4935.
26. Xu L, Jiang Q, Xiao Z, Li X, Huo J, Wang S, Dai L, Plasma-engraved Co3O4 nanosheets with oxygen vacancies and high surface area for the oxygen evolution reaction. *Angewandte Chemie*, 2017; *128* (17): 5363-5367.

27. Wang D, Wang Q, Wang T, Morphology-controllable synthesis of cobalt oxalates and their conversion to mesoporous Co3O4 nanostructures for application in supercapacitors. J. Inorg. Chem. 2011 *50* (14): 6482-6492.

28. Xia X H, Tu J P, Zhang Y Q, Mai Y J, et. al. Freestanding Co3O4 nanowire array for high performance supercapacitors. Rsc Advances, 2012; 2(5): 1835-1841.

29. Zheng M B, Cao J, Liao S T, et. al. Preparation of mesoporous Co3O4 nanoparticles via solid–liquid route and effects of calcination temperature and textural parameters on their electrochemical capacitive behaviors. J. Tao, Phys. Chem. C 2009; 113 (9): 3887.

30. Wang L, Liu X H, Wang X, et. al. Preparation and characterization of mesoporous Co3O4 electrode material. J. Appl. Phys. 2010; 10 1422.

31. Asano Y, Komatsu T, Murashiro K, et al. Capacitance studies of cobalt compound nanowires prepared via electrodeposition. J. Power Source 2011; 196 (11): 5215-5222.

32. Wen W, Wu J, M, & Tu J P, A novel solution combustion synthesis of cobalt oxide nanoparticles as negative-electrode materials for lithium-ion batteries. *Journal of alloys and compounds*, 2012; *513* 592-596.

33. Manish A K, Subramania K B, Preparation of electrospun Co3O4 nanofibers as electrode material for high performance asymmetric supercapacitors. J. Electrochimica Acta. 2014; 149 152-158.

34. Suryanto B H, Wang Y, Hocking R K, Adamson W, & Zhao C, Overall electrochemical splitting of water at the heterogeneous interface of nickel and iron oxide. *Nature communications*, 2019; *10*(1): 1-10. 35**.** Jang H, Yang Y, SukLee N, et al. Electrospun RuO2–Co3O4 hybrid nanotubes for enhanced electrocatalytic activity**.** J. Materials Letters 2015**;** 139 405**-**408.

36. Mugheri A Q, Tahira A, Aftab U, et al. An advanced and efficient Co 3 O 4/C nanocomposite for the oxygen evolution reaction in alkaline media. J. RSC Adv. 2019; 9 34136-34143.

37. Anantharaj S, Karthick K, Kundu S, Evolution of layered double hydroxides (LDH) as high-performance water oxidation electrocatalysts: A review with insights on structure, activity, and mechanism. J. Mater Today Energy 2017; 6 1-26.

38. Browne M P, Nolan H, Duesberg G S, et al. Low-overpotential high-activity mixed manganese and ruthenium oxide electrocatalysts for oxygen evolution reaction in alkaline media. J. ACS Catalst 2016; 6 2408-2415.

39. Doyle R L, Godwin I J, Brandon M P, et al. Redox and electrochemical water splitting

catalytic properties of hydrated metal oxide modified electrodes. J. Chem Phys. 2013; 15 (33): 13737-13783.

40. Zou L, and Xu Q, Synthesis of a hierarchically porous C/Co3O4 nanostructure with boron doping for oxygen evolution reaction. J. Chemistry - An Asian Journal 2020; 15 (4) 490-493.

41. Aftab U, Tahira A, Samo A H, et al. Mixed CoS2@ Co3O4 composite material: An efficient nonprecious electrocatalyst for hydrogen evolution reaction. J. International Journal of Hydrogen Energy 2020 45 (27); 1380513813.

42. Song F, and Hu X, Exfoliation of layered double hydroxides for enhanced oxygen evolution catalysis. J. Nature Communications 2014; 5 (1): 4477.

[43] Jin H, Wang J, Su D, et al. In situ cobalt–cobalt oxide/N-doped carbon hybrids as superior bifunctional electrocatalysts for hydrogen and oxygen evolution. J. Am. Chem. Soc. 2015; 137 2688-2694.

44. Zhang Y, Xiao J, Lv Q, & Wang S, Self-supported transition metal phosphide based electrodes as high-efficient water splitting cathodes. *Frontiers of Chemical Science and Engineering*, 2018; *12* (3): 494-508. [45] Song F and Hu X, Ultrathin cobalt–manganese layered double hydroxide is an efficient oxygen evolution catalyst. J. Am. Chem. Soc 2014; 13 (47):16481-16484.

46. Liang Y, Li Y, Wang H, et al. Co 3 O 4 nanocrystals on graphene as a synergistic catalyst for oxygen reduction reaction. J. Nature Materials 2016; 10 (10): 780-786.

47. McCrory C C, Jung S, J Peters. Benchmarking heterogeneous electrocatalysts for the oxygen evolution reaction. J. Am. Chem. Soc. 2013; 13 (45): 26 28.

48. Cui X, Ren P, Deng D, et al. Single layer graphene encapsulating non-precious metals as high-performance electrocatalysts for water oxidation. J. Energy Environ. Sci. 2013; 9 (1):123 129.

49. Li Y, Hasin P, & Wu Y, NixCo3− xO4 nanowire arrays for electrocatalytic oxygen evolution. *Advanced materials*. 2010; *22* (17), 1926-1929.

50. Song F, & Hu X, Exfoliation of layered double hydroxides for enhanced oxygen evolution catalysis. J. Nat. Commun. 2014; 5 (1): 4477 83.

51. Lu X F, Liao P Q, Wang J W, et al. An alkaline-stable, metal hydroxide mimicking metal–organic framework for efficient electrocatalytic oxygen evolution. J. Am. Chem. Soc. 2016; 138 (127): 8336 8339.

52. Liang Y, Li Y, Wang H, et al. Co 3 O 4 nanocrystals on graphene as a synergistic catalyst for oxygen reduction reaction. *Nature materials* 2011; *10* (10): 780-786.

53. Wan Z, Yu H, He Q, Hu Y, et. al. In-situ growth and electronic structure modulation of urchin-like Ni–Fe oxyhydroxide on nickel foam as robust bifunctional catalysts for overall water splitting. *International Journal of Hydrogen Energy*, 2020; *45*(43): 22427-22436.

54. Zhang Z G, Li H, Qi B, Chi D, Jin Z, Qi Z, et. al. Amine group functionalized fullerene derivatives as cathode buffer layers for high performance polymer solar cells. *Journal of Materials Chemistry A*, 2013. *1*(34): 9624-9629.

55. Song F, & Hu X, Exfoliation of layered double hydroxides for enhanced oxygen evolution catalysis. J. Nat. Commun, 2014; *5*(1): 1-9.

56. Zhong-Li W, Xian-Feng, Zheng J, et al. "C and N hybrid coordination derived Co–C–N complex as a highly efficient electrocatalyst for hydrogen evolution reaction. J. Am. Chem. Soc. 2015; 48 15070-15073.

57. Jin H, Wang J, Su D, et al. Co 3 O 4 nanocrystals on graphene as a synergistic catalyst for oxygen reduction reaction. J. Nat. Mater. 2011; 10 (10): 780-786.

58. Li Y, Hasin P, Wu Y, NixCo3− xO4 nanowire arrays for electrocatalytic oxygen evolution. J. Adv. Mater. 2010; 22 (17): 1926-1929.

59. Huang T, Mao S, Zhou G, Wen Z, Huang X, Ci S, & Chen J, Hydrothermal synthesis of vanadium nitride and modulation of its catalytic performance for oxygen reduction reaction. *Nanoscale*, 2014; *6*(16): 9608-9613.

Figure Captions

Figure 1. Schematic diagram showing the synthesis process and electrochemical analysis

Figure 2. a. pristine Co_3O_4, b. Co_3O_4/PVP, c. nanofiberes of PVP, d. XRD for pristine Co_3O_4 and Co_3O_4/PVP

Figure 3. Elemental mapping and EDS spectra of Co_3O_4/PVP

Figure 4. a. LSV curves at scan rate of 1 mV/s of pristine Co_3O_4, Co_3O_4/PVP, PVP fibers, 20%RuO_2/C in 1.0M KOH, b. Tafel plots, c. chronopotentiometry experiment at 20 $mAcm^{-2}$ for 20 h, d. stability before and after the durability test

Figure 5. (a-b) CV curves of pristine Co_3O_4, and Co_3O_4/PVP at different scan rates in 1.0M KOH, **c.** Linear fitting of current density versus scan rate for the calculation of Cdl of pristine Co_3O_4, and Co_3O_4/PVP

Figure 6.EIS spectra for pristine Co_3O_4 and Co_3O_4/PVP, at 100 KHz to 1Hz, amplitude 5 mV and OER onset potential in 1.0M KOH, **a.b**. Bode plots, **c.** Corresponding Nyquist plots

Figure 1

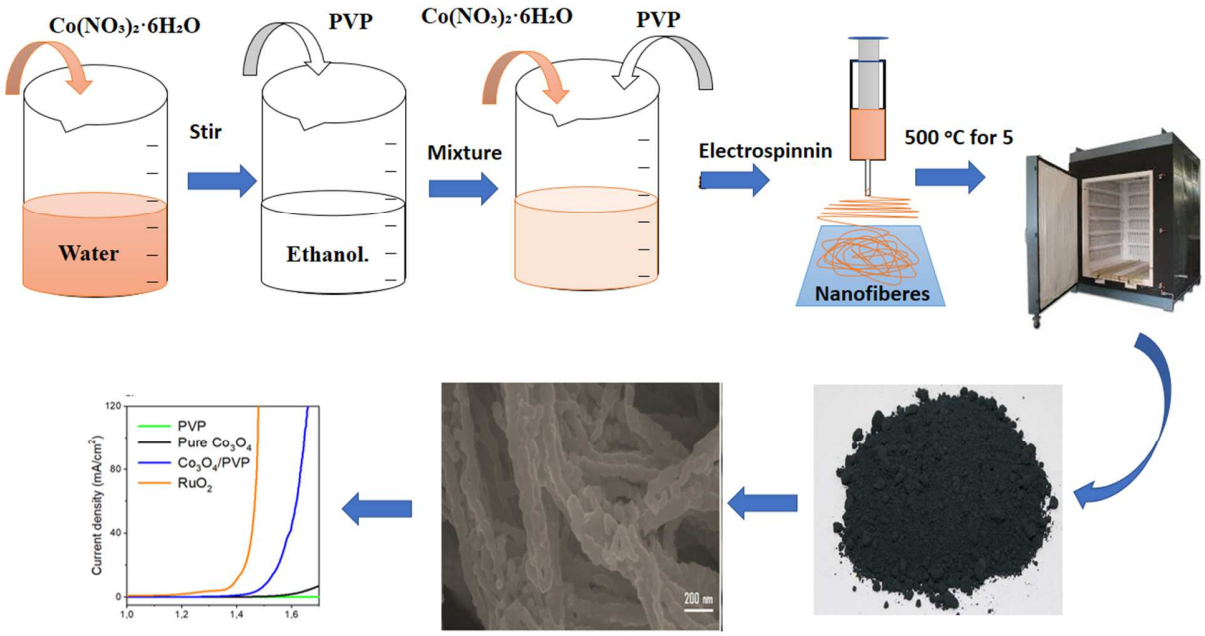
Co(NO3)2·6H2O
Water
Stir
PVP
Ethanol.
Co(NO3)2·6H2O
Mixture
PVP
Electrospinnin
Nanofiberes
500 °C for 5
PVP
Pure Co3O4
Co3O4/PVP
RuO2
Current density (mA/cm2)
200 nm

Figure 2

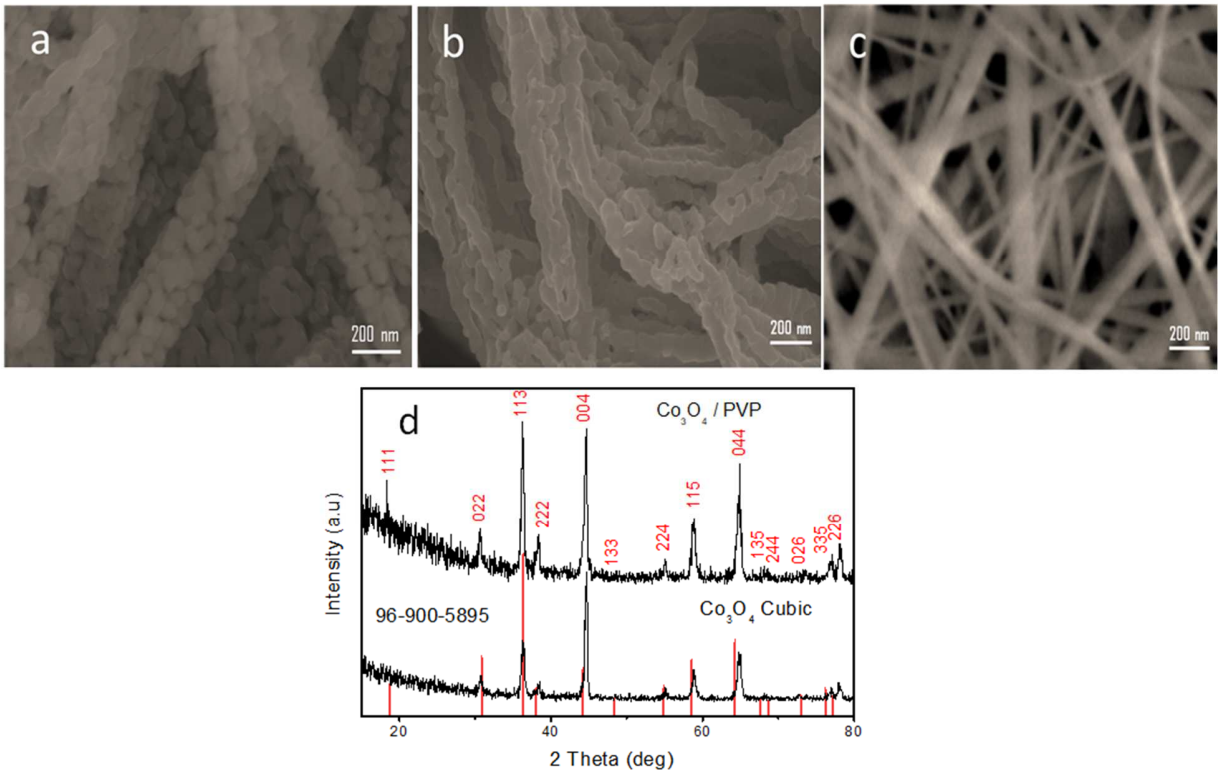
a
200 nm
b
200 nm
c
200 nm
d
Co3O4 / PVP
111
022
113
222
004
133
224
115
044
135
244
026
335
226
96-900-5895
Co3O4 Cubic
Intensity (a.u)
20
40
60
80
2 Theta (deg)

Figure 3

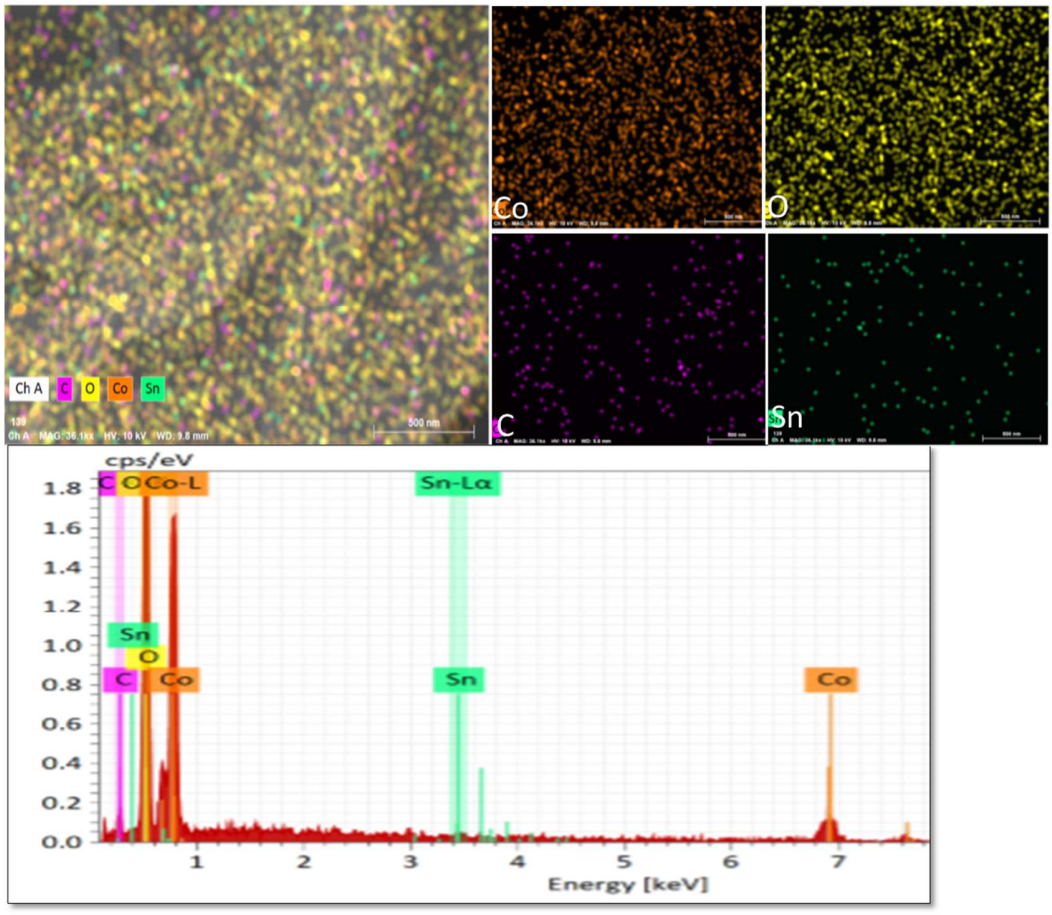
Ch A
C
O
Co
Sn
500 nm
Co
O
C
Sn
cps/eV
C
O
Co-L
Sn-Lα
Sn
O
C
Co
Sn
Co
1.8
1.6
1.4
1.2
1.0
0.8
0.6
0.4
0.2
0.0
1
2
3
4
5
6
7
Energy [keV]

Figure 4

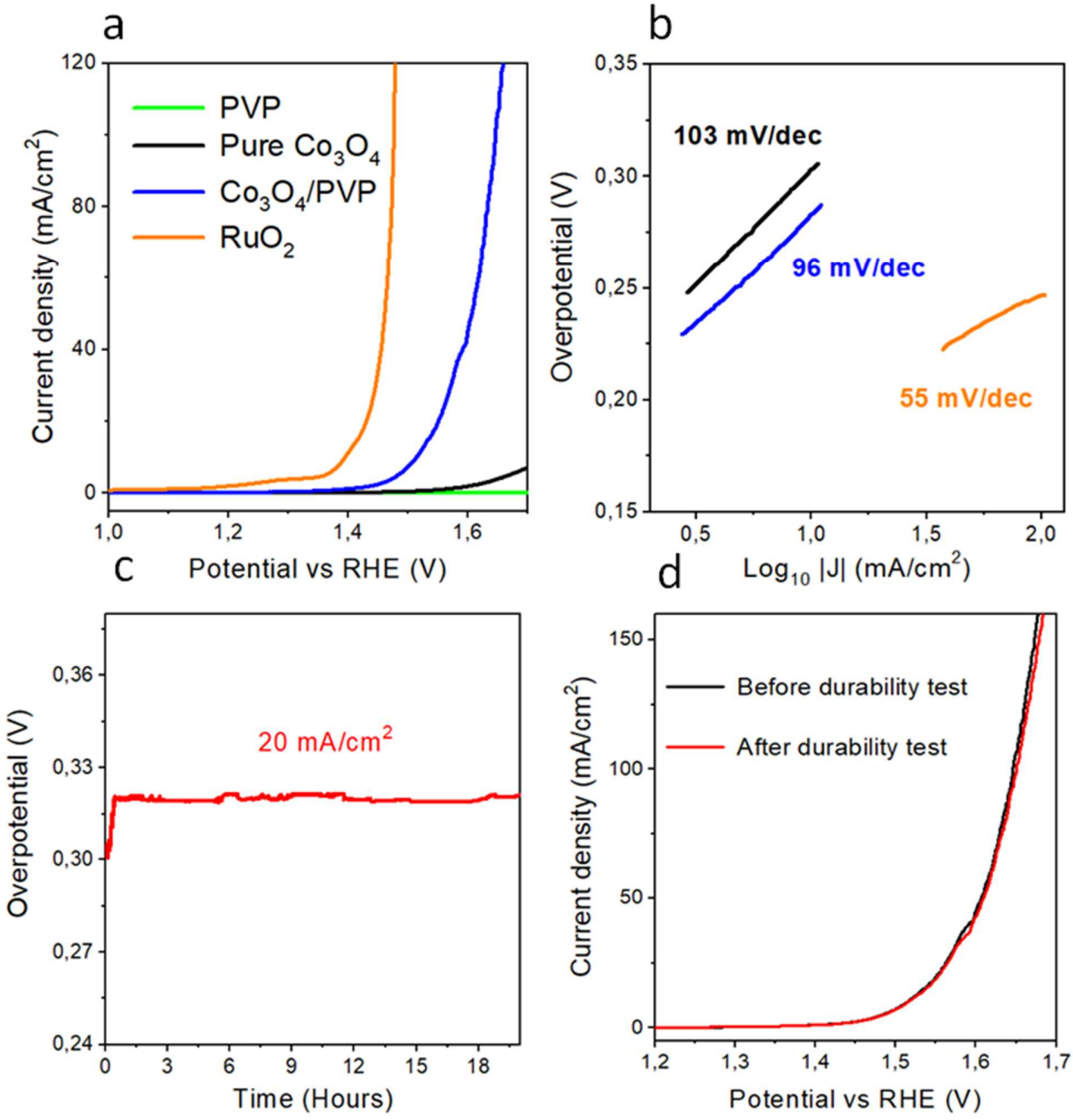
a
Current density (mA/cm^2)
120
80
40
0
1,0
1,2
1,4
1,6
Potential vs RHE (V)
PVP
Pure Co_3O_4
Co_3O_4/PVP
RuO_2
b
Overpotential (V)
0,35
0,30
0,25
0,20
0,15
0,5
1,0
1,5
2,0
Log_{10} |J| (mA/cm^2)
103 mV/dec
96 mV/dec
55 mV/dec
c
Overpotential (V)
0,36
0,33
0,30
0,27
0,24
0
3
6
9
12
15
18
Time (Hours)
20 mA/cm^2
d
Current density (mA/cm^2)
150
100
50
0
1,2
1,3
1,4
1,5
1,6
1,7
Potential vs RHE (V)
Before durability test
After durability test

Figure 5

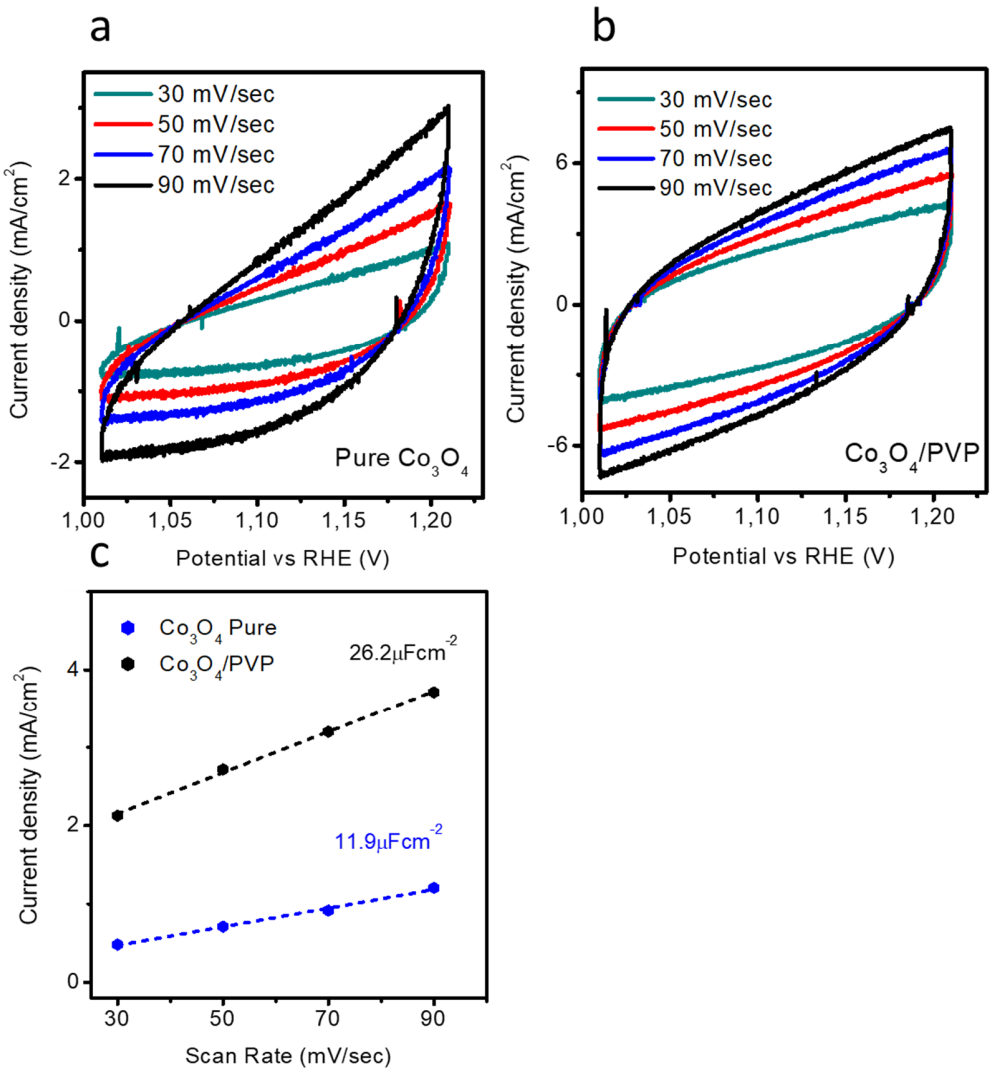
a
30 mV/sec
50 mV/sec
70 mV/sec
90 mV/sec
Pure Co3O4
Current density (mA/cm2)
Potential vs RHE (V)
b
Co3O4/PVP
c
Co3O4 Pure
Co3O4/PVP
26.2μFcm-2
11.9μFcm-2
Scan Rate (mV/sec)

Figure 6

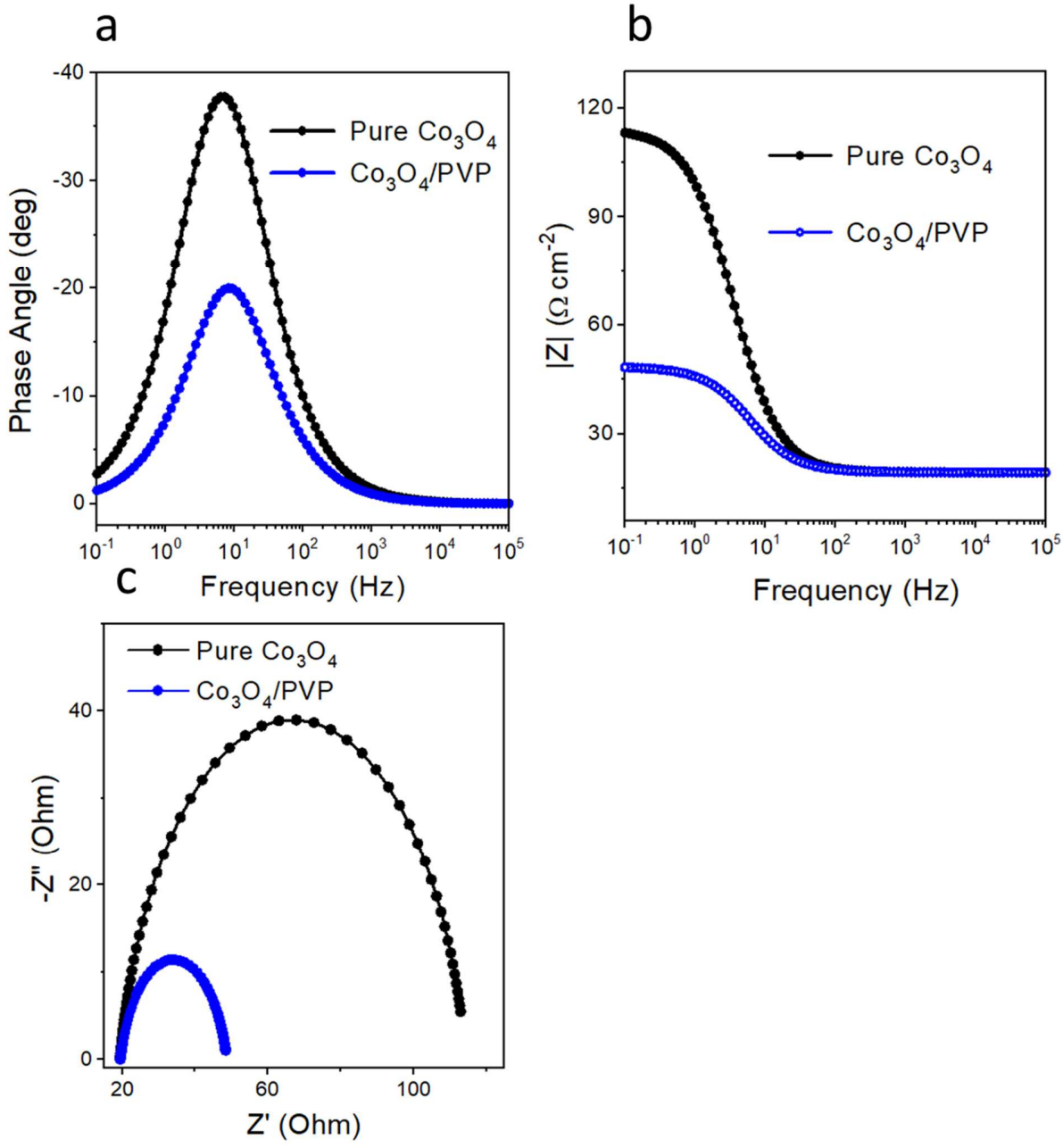
a
Phase Angle (deg)
-40
-30
-20
-10
0
Pure Co_3O_4
Co_3O_4/PVP
10^{-1} 10^{0} 10^{1} 10^{2} 10^{3} 10^{4} 10^{5}
Frequency (Hz)
b
|Z| (Ω cm^{-2})
120
90
60
30
Pure Co_3O_4
Co_3O_4/PVP
10^{-1} 10^{0} 10^{1} 10^{2} 10^{3} 10^{4} 10^{5}
Frequency (Hz)
c
-Z'' (Ohm)
40
20
0
Pure Co_3O_4
Co_3O_4/PVP
20
60
100
Z' (Ohm)

Table 1. EIS fitting values for the circuit elements

Catalyst	Rct (Ohm)	Cdl (mF)
Co_3O_4	94.98	0.68
Co_3O_4 nanofibers	29.23	1.11

Table 2. Comparison of presented Co_3O_4 nanoparticles deposited on PVP fibers with various published results.

Catalyst	Overpotential mV	Tafel slope mV dec^{-1}	Reference
CoCo LDH	393	59	38
CoOx@CN	~385	N/A	39
Co-P films	345	47	40
$MnCo_2Ox$	>410	84	41
Co_3O_4/N-rmGO	310	67	42
NiCoOx	420	N/A	43
N-G-CoO	340	71	44
$NixCo_3$-xO	~370	59~64	45
CoCo LDH	393	59	46
CoO_x@CN	~385	--	47
Co-P films	345	47	48
$NixCo_3$-xO	~370	59~64	49
$NixCo_3$-xO	~370	59-64	50
CoCo LDH	393	59	51
CoOx@CN	~385	N/A	52

Co-P films	345	47	53
$MnCo_2Ox$	>410	84	54
Co_3O_4/N-rmGO	310	67	55
Carbonized Co_3O_4	280	96	**Present work**